Photorefractive detection of tissue optical and mechanical properties by ultrasound modulated optical tomography

Xiao Xu

Optical Imaging Laboratory, Department of Biomedical Engineering, Texas A&M University, College Station, Texas 77843, USA

Huiliang Zhang and Philip Hemmer

Department of Electrical and Computer Engineering, Texas A&M University, College Station, Texas 77843, USA

De-kui Qing

Institute for Quantum Studies and Department of Physics, Texas A&M University, College Station, Texas 77843, USA

Chulhong Kim and Lihong V. Wang

Optical Imaging Laboratory, Department of Biomedical Engineering, Texas A&M University, College Station, Texas 77843, USA

Received September 11, 2006; revised November 17, 2006; accepted December 12, 2006; posted December 15, 2006 (Doc. ID 74954); published February 15, 2007

Ultrasound-modulated optical tomography is a developing hybrid imaging modality that combines high optical contrast and good ultrasonic resolution for imaging soft biological tissue. We developed a photorefractive-crystal-based, time-resolved detection scheme with the use of a millisecond long ultrasound burst to image both the optical and the mechanical properties of biological tissues, with improved detection efficiency of ultrasound-tagged photons. © 2007 Optical Society of America

OCIS codes: 170.0170, 190.0190, 190.5330.

Ultrasound-modulated optical tomography (UOT) is a promising hybrid imaging technique for biological tissue. In UOT a focused ultrasound beam interacts with diffused light by means of phase modulation inside a biological sample. Detection of the ultrasound modulated (or tagged) photons enables one to recover the spatial distribution of the optical properties inside the sample, which are often of biomedical interest. Various research groups have made contributions to the theoretical and experimental development in this field.[1–7] In recent years photorefractive-crystal (PRC) based detection has been applied to UOT, which effectively improves the etendue of the imaging system based on PRC's real-time holography feature in a two-wave mixing (TWM) or four-wave mixing scheme. Several variations of the PRC-based UOT system have been implemented and the relevant theories developed by various groups.[8–11]

We propose a PRC-based UOT system with a quasi-continuous-wave (CW) ultrasound-modulation scheme, where a 1 ms long focused ultrasound burst was applied to the sample and the time dependent change of the detected optical signal was recorded to image both the optical and the mechanical properties of the sample. The benefits of using a millisecond long ultrasound burst are twofold: it improves the SNR, and it also allows the detection of the effects of the acoustic radiation force, which happens on a millisecond time scale and can be related to the mechanical properties of the sample.

Our experiment setup, shown in Fig. 1, was similar to what was proposed by Murray *et al.*[8] The light from a Coherent Verdi laser ($\lambda = 532$ nm) was split into two paths: one (signal) for illuminating the sample and the other for pumping in two-wave mixing in the PRC. The sample was insonified by a focusing ultrasonic transducer (Ultran Lab VHP 100-1-R38) with a central frequency of 1 MHz, focal length of 37.5 mm, focal zone length of 23 mm, and focal spot diameter of 2.2 mm. The peak acoustic pressure at the focus was 1.5 MPa. The high amplitude of the ultrasound burst was compensated by its low duty cycle (burst rate was 100 Hz) so that the ultrasound

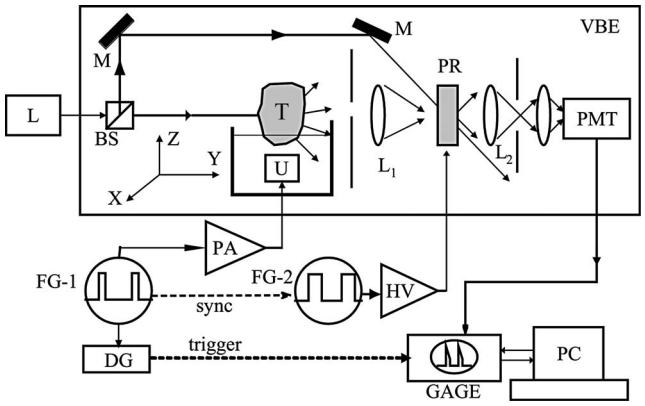

Fig. 1. Schematic of the experiment setup: L, laser; BS, beam splitter; M, mirror; L_1, L_2, lens; PR, photorefractive crystal BSO; PMT, photomultiplier; FG-1, FG-2, function generators; PA, power amplifier; DG, pulse-delay generator; HV, high voltage amplifier; PC, personal computer; U, 1 MHz ultrasound transducer; T, study sample; VBE, vibration block enclosure; GAGE, CompuScope 14200 14 bit waveform digitizer.

0146-9592/07/060656-3/$15.00

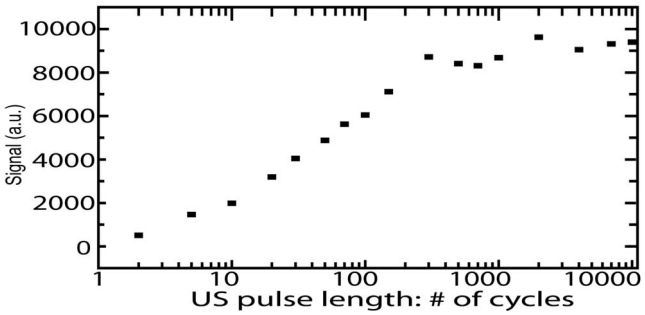

Fig. 2. Signal intensity grows as the burst length increases. US, ultrasound.

safety limit was still satisfied.[12] An alternating electric field (1 kHz, 4 kV) was applied to the BSO crystal to enhance the TWM gain. The pump light intensity incident on the BSO was kept around 10 mW/cm^2. Under this condition, we measured that the crystal response time was at least 100 ms, which was comparable with the speckle decorrelation time of 2 cm *ex vivo* chicken breast tissue.[13] The system was enclosed in an acrylic enclosure to prevent the real-time holography from undergoing perturbations.

To quantify the improvement of UOT signal strength with increasing ultrasound burst duration, a phantom sample (sample 1) was prepared with 10% porcine gelatin and 1% Intralipid concentration, resulting in a reduced scattering coefficient $\mu_s' = 10\ \mathrm{cm}^{-1}$, and 10 cm $\times$ 4 cm $\times$ 10 cm ($X \times Y \times Z$) outer dimensions. Ultrasound bursts consisting of various numbers of cycles were applied to the phantom, and light intensities after the BSO were registered by the photomultiplier. The signal strength was defined as the change in detected light intensity with and without ultrasound modulation. Figure 2 shows the signal increase and saturation as the ultrasound burst length increases. Several possible mechanisms can account for this. (1) The increasing ultrasound burst duration fills a larger sample volume along the Z axis, which increases the amount of ultrasound-modulated light at the expense of axial resolution. (2) The momentum transfer in the ultrasound focal zone increases with the increasing ultrasound duration because of the radiation force effect,[14] which increases the ultrasound modulation of light in the focal zone. (3) The TWM response time in BSO due to the intensity change of the unmodulated light is comparable with this time scale.

We took advantage of the higher signal levels provided by long ultrasound burst to image chicken gizzard pieces embedded in chicken breast tissue (sample 2, Fig. 3). The two chicken gizzard pieces, each 6 mm $\times$ 6 mm $\times$ 10 mm, were separated 10 mm apart inside an 8 cm $\times$ 2.5 cm $\times$ 3.8 cm chicken breast sample, which was buried in 10% porcine gel with the same outer dimensions as sample 1. Chicken gizzard has higher optical absorption than the surrounding chicken breast tissue but similar mechanical properties. This translates into less ultrasound-modulated light inside the chicken gizzards, and hence less change of the unmodulated light, or a decrease in UOT signal. This was illustrated by the two dark troughs at the locations of the two gizzards as seen in the 2D images in Fig. 3.

To demonstrate imaging based on mechanical properties, rather than optical properties, a phantom sample (sample 3) was prepared with the same composition and outer dimensions as sample 1 but having two 6 mm cubic volumes enhanced with 20% corn starch as buried objects with a 12 mm separation. The two inclusions had minimal differences in optical properties but a higher mechanical contrast than the background. As a result, the inclusions were barely discernible on the UOT image acquired 0.1 ms after the onset of the ultrasound burst (Fig. 4, upper plot) but were markedly visible on the image acquired 0.1 ms after the passage of the ultrasound burst (Fig. 4, lower plot), because the mechanical property dif-

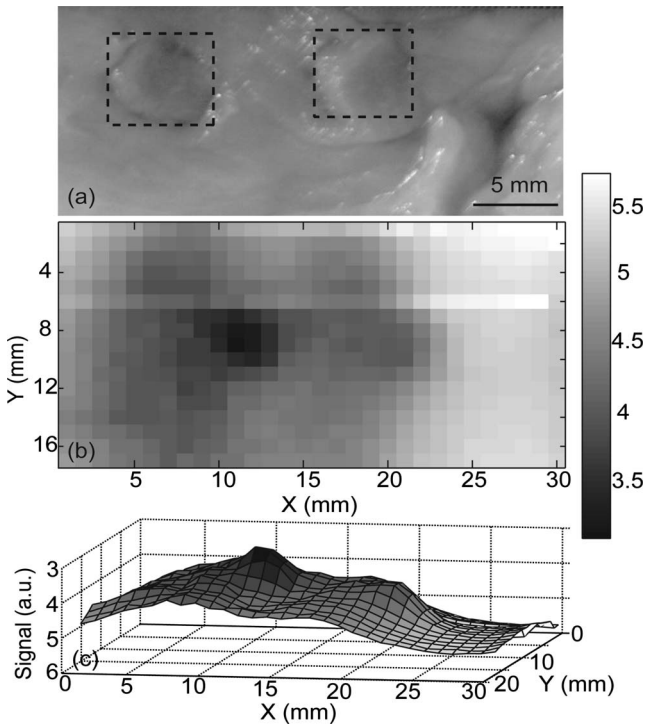

Fig. 3. UOT image of sample 2. (a) Picture of the sample; (b), (c) density and surface map of the 2D UOT image of (a); the surface map is upside down to show the objects.

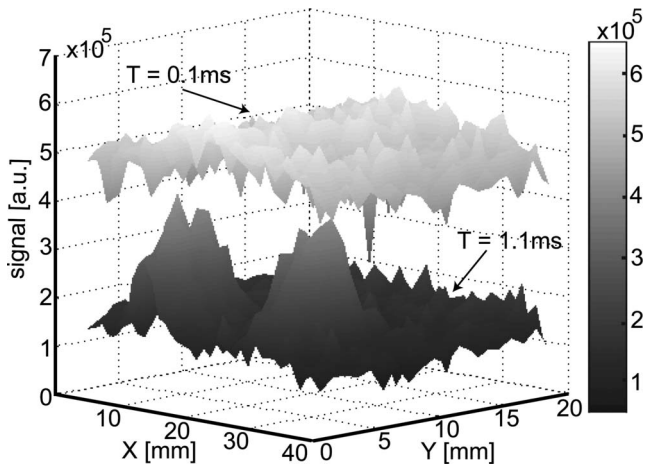

Fig. 4. UOT surface maps sample of 3 at $T = 0.1$ ms and 1.1 ms after the start of a 1 ms long ultrasound burst.

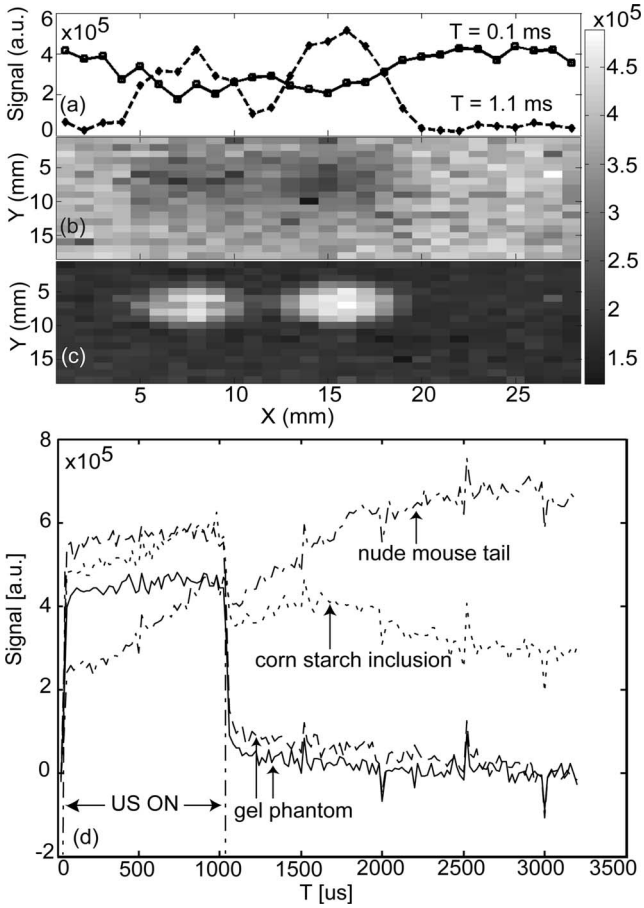

Fig. 5. (a) 1D scan at $y = 7$ mm of sample 4; (b), (c) 2D density map at (b) $T = 0.1$ ms and (c) $T = 1.1$ ms; (d) comparison of time-resolved UOT signal for various objects.

ferences gave rise to the acoustic radiation force effect that happened on a time scale of several milliseconds.[14]

We next demonstrated UOT imaging based on both optical and mechanical properties by imaging two segments of nude mouse tail, with 3 mm × 10 mm (diameter × Z) in dimension and 8 mm separation, embedded in a gelatin sample (sample 4) with the same composition and outer dimension as sample 1. The UOT image [Fig. 5(b)] acquired at $T = 0.1$ ms after the onset of the ultrasound was based mainly on optical absorption contrast. Owing to the higher absorption of the mouse tails, they appear dark, but the contrast is low. The image quality is much better for ultrasound light modulation produced by the radiation force effect, because of the large acoustic impedance mismatch between the bone structures of the nude mouse tail and the background gelatin phantom. This is shown in Fig. 5(c), where the image was acquired 0.1 ms after the end of the 1 ms ultrasound. Here the mouse tails appear bright owing to strong acoustic modulation. The 1D scans [Fig. 5(a)] across the sample at the two different times show the different effects of optical and mechanical contrasts on the UOT signal.

Details of the mechanical properties of the object, such as the acoustic impedance mismatch, can be characterized from the time-evolution curves of the UOT signal. To demonstrate this, a comparison of time-evolution curves from the nude mouse tail, the corn starch inclusion, and their background gelatin phantoms are shown in Fig. 5(d). For the nude mouse tail, the radiation force effect kept increasing long after the ultrasound was turned off, while for the corn starch inclusion it started decay 0.5 ms after the end of the ultrasound burst. For both samples the background gelatin curves showed little radiation force effect, as expected. Separation of the sample's mechanical and optical contrast is possible once the acoustic impedance can be derived from the time-resolved UOT imaging.

In summary, this study has demonstrated that both the optical properties and the acoustic radiation force effect can be detected with a millisecond ultrasound burst, using PRG-based UOT. Time gating the optical signal even allows decoupling of optical and mechanical information from UOT. Finally, the signal-to-noise ratio can also be improved with a longer ultrasound burst.

We thank Sava Sakadžić and Roger Zemp for fruitful scientific discussions. This research was supported by the National Institutes of Health grant R33 CA 094267 and Air Force Office of Scientific Research grant FA9550-04-1-0247. L. Wang's e-mail address is lwang@bme.tamu.edu.

References

1. F. A. Marks, H. W. Tomlinson, and G. W. Brooksby, Proc. SPIE **1888**, 500 (1993).
2. L.-H. Wang, S. L. Jacques, and X. Zhao, Opt. Lett. **20**, 629 (1995).
3. S. Leveque, A. C. Boccara, M. Lebec, and H. Saint-Jalmes, Opt. Lett. **24**, 181 (1999).
4. S. Sakadzic and L.-H. Wang, Opt. Lett. **29**, 1 (2004).
5. M. Kempe, M. Larionov, D. Zaslavsky, and A. Z. Genack, J. Opt. Soc. Am. A **14**, 1151 (1997).
6. S. Sakadzic and L.-H. Wang, Phys. Rev. E **66**, 026603 (2002).
7. S. Sakadzic and L.-H. Wang, Phys. Rev. E **72**, 036620 (2005).
8. T. W. Murray, L. Sui, G. Maguluri, R. A. Roy, A. Nieva, F. Blonigen, and C. A. DiMarzio, Opt. Lett. **29**, 2509 (2004).
9. F. Ramaz, B. C. Forget, M. Atlan, A. C. Boccara, M. Gross, P. Delaye, and G. Roosen, Opt. Express **12**, 5469 (2004).
10. E. Bossy, L. Sui, T. W. Murray, and R. A. Roy, Opt. Lett. **30**, 744 (2005).
11. M. Gross, F. Ramaz, B. C. Forget, M. Atlan, C. Boccara, P. Delaye, and G. Roosen, Opt. Express **13**, 7097 (2005).
12. American Institute of Ultrasound in Medicine, "Mammalian *in vivo* ultrasonic biological effects" (1992), http:///www.aium.org.
13. G. Yao and L.-H. Wang, Appl. Opt. **43**, 1320 (2004).
14. K. Nightingale, R. Nightingale, M. Palmeri, and G. Trahey, Ultrason. Imaging **22**, 35 (2000).